Femtosecond laser processing of maraging steel fabricated by laser powder bed fusion

WCMNM 2021

Balasubramanian Nagarajan, Jitka Metelkova, Jide Han, Brecht Van Hooreweder, Sylvie Castagne

KU Leuven, Department of Mechanical Engineering and Flanders Make@KU Leuven-MaPS, Celestijnenlaan 300, 3001 Leuven, Belgium

Abstract

Recently, femtosecond (*fs*) lasers are finding increasing attention as a post-AM surface finishing process due to the minimal thermal effects and ability to fabricate submicron surface textures. In this manuscript, we investigate the effects of direct femtosecond laser processing (FLP) of surfaces produced by laser powder bed fusion (LPBF). Maraging steel 300 was used as the substrate material. FS laser experiments were performed on samples with different initial surface conditions including as-built LPBF and laser polished with continuous wave and pulsed lasers. The study focuses on the influence of process parameters such as laser pulse energy, scanning speed and number of scanning passes on the surface texture. The processed surfaces are analysed using confocal microscope and scanning electron microscopy. The results indicate that FLP of LPBF parts improve the surface finish and produce LIPSS features with a periodicity of 500 nm. The presence of spatter particles on the surface can be addressed through FLP process optimization and adoption of different scanning strategies for surface finishing and texturing.

Keywords: Laser powder bed fusion, femtosecond laser processing, laser surface texturing, AM post-processing

1. Introduction

Despite the commercialization of AM techniques such as laser powder bed fusion (LPBF) in the aerospace and biomedical industry [1], AM is still focussed on macroscale components. Adoption of LPBF for microscale applications is restricted by limited feature resolution, inability to process fine powder particles and part defects [2].

Poor surface finish is one of the major limitations of AM techniques. The parts fabricated by LPBF typically require post-process finishing as the arithmetic mean surface roughness (R_a) is generally higher than 10 µm [2]. Laser polishing (LP) or remelting is emerging as a promising in-situ post-AM surface finishing technique [3,4]. It is based on the redistribution of surface peaks into the valleys due to melt pool surface tension. Kruth et al. [5] demonstrated that laser remelting can significantly improve surface roughness of LPBF-fabricated 316L surfaces (from R_a=12 µm to 1.5 µm). Besides horizontal top surfaces, *ns*-pulsed laser was recently used to improve the roughness of up-facing inclined surfaces during LPBF through in-situ laser surface remelting combined with laser-induced shockwaves [6].

Nowadays, femtosecond (*fs*) lasers are finding increasing application as a post-AM surface finishing process [7–10]. Mingareev et al. [7] first used *fs* laser machining to reduce surface roughness (R_a) of LPBF top samples from 22 µm to 3 µm through multilayer processing with varying offset distance along Z-axis. A recent study on *fs* laser micromachining of LPBF Ti6Al4V specimen reported a reduction in R_a from 4.23 µm to 0.8 µm through single pass raster scanning [9]. Besides the top surface, in recent studies [8,10], *fs* lasers were used to significantly improve surface finish of LPBF side-walls.

Typically, *fs* lasers are used for laser surface texturing (LST) to alter the surface characteristics including adhesion, friction, wettability, biocompatibility and optical response [11]. During ultrashort pulse irradiation with laser fluence near the ablation threshold, laser-induced periodic surface structures (LIPSS) or ripples, up to the scale of sub-wavelength periodicity, can be fabricated using *fs* lasers. Worts et al. [9] first reported the formation of micro-conical structures and nanogratings after *fs* laser processing of LPBF surfaces, but there was no information on the uniformity of the fabricated patterns. Batal et al. [12] investigated laser polishing (using *ns*-pulsed laser) followed by LST (using *fs* laser) of freeform LPBF Ti6Al4V surfaces. LST of laser-polished LPBF planar surface resulted in sub-micron ripples with a periodicity of 860 nm [12]. It was highlighted that laser polishing of AM surfaces before LST is essential in order to achieve uniform LIPSS structures [12].

However, in comparison to *fs* laser processing, laser polishing using *ns* lasers typically cause larger heat affected zone, thermal stresses, microstructural changes, surface cracks and inclusions [3,4]. Thermal stresses could lead to distortions or damage which will affect the part integrity. This is especially true for microscale parts such as thin-walls [2,7], which underlines the need for direct ultrashort laser pulse processing. Despite the recent published research [9,12], there are no extensive studies on the optimization of LST process for as-built LPBF parts.

The aim of this work is to improve the LPBF surface finish and tailor the surface texture. Therefore, the effect of direct *fs* laser processing on finishing and texturing of LPBF part surfaces is studied. Femtosecond laser processing (FLP) of four different initial process conditions (as-built LPBF, laser polished and mechanically ground) is evaluated. The effect of various FLP process variables such as laser pulse energy, scanning speed and the number of scanning passes on the surface topography is analysed in detail.

2. Materials and methods

2.1. Laser powder bed fusion (LPBF) and laser polishing (LP) of maraging steel

AM samples were manufactured using a modified LPBF machine from 3D Systems (ProX DMP 320A) which consists of a continuous wave (CW) fiber laser

Table 1. Process conditions for LPBF and laser polishing (LP) experiments*

Samples	Condition	LPBF parameters	Laser polishing parameters						
			P (W)	PRR (kHz)	τ (ns)	ν (mm/s)	Repetitions	*h* (μm)	Defocus (mm)
S1 (as-built)	LPBF	P = 150W ν =1100 mm/s *h* =70um *t* =30um				N.A			
S2 (LPBF+MG)	Mechanically ground (MG)					N.A			
S3 (LPBF+LP1)	LP using *ns*-pulsed laser		45 W	1000	30	1250	40x	10	0
S4 (LPBF+LP2)	LP using CW laser		230 W	NA	NA	800	10x	35	2

* PRR – pulse repetition rate, ν - scanning speed, τ - pulse duration, *t* – layer thickness, *h* - hatch spacing

with a maximum output power of 500 W, central wavelength (λ) of 1070 nm and spot size (d_{1/e^2}) of 60 μm. For laser polishing (LP), an Ytterbium fiber ns pulsed laser [max. average power (P_{avg}) = 50 W, max. pulse energy (E_p) = 520 μJ at a pulse duration (τ) of 30 ns, λ = 1070 nm, spot size d_{1/e^2} = 50 μm] is integrated. The LPBF machine has a single scanner and a flipping optic to enable switching between the CW laser and *ns*-pulsed laser. Maraging steel 300 powder with a particle size distribution of 15 - 45 μm was used to fabricate 30 mm x 10 mm samples. In order to acquire different initial surface conditions for FLP, samples with different process flows were selected. Table 1 summarizes the LPBF and LP process parameters used. The selection of parameters for LPBF and LP is based on our previous research works published in [6] and [13]. Both LPBF and LP experiments were performed under inert argon atmosphere. The scanning strategy was bidirectional, for LPBF under 45° to the part edge and for LP parallel to the shorter sample dimension. Fig. 1 shows the top surface of as-built and laser polished samples and the metallographic cross-sections in the vicinity.

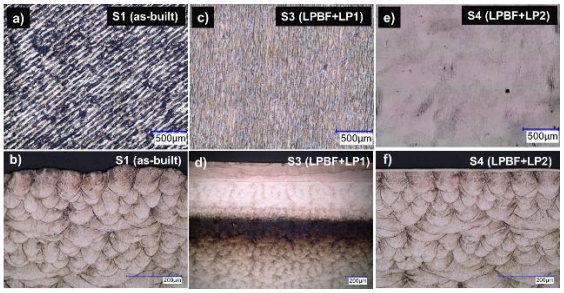

Fig. 1. Surface & cross-sectional morphology of S1 [as-built LPBF] (a,b), S3 [LPBF+LP1] (c,d) and S4 [LPBF+LP2] (e,f)

2.2. Femtosecond laser processing (FLP)

FLP was conducted using a *fs* laser (SATSUMA) from Amplitude Systèmes with a Gaussian beam. The specification of the system is as follows: pulse duration (τ) = 250 *fs*, maximum average laser power = 10 W, maximum pulse energy (E_p) = 20 μJ, spot size (d_{1/e^2}) = 16 μm and focal length = 100 mm. Laser processing is conducted on the top surface (surface normal to the build direction) of the LPBF samples. A constant pulse repetition rate (PRR) of 500 kHz and a bidirectional scanning strategy with a hatch spacing of 5 μm were used for all the experiments.

Table 2. Process parameters used for FLP

Process parameters	Values
Laser pulse energy (E_p) (μJ)	4.5, 7.5, 10.9, 14, 16
Scanning speed (ν) (mm/s)	100, 200, 400, 800, 1600
Number of passes (*N*)	1, 2, 3, 4

2.3. Surface characterization

Surface topography and roughness were characterized using a confocal microscope, Sensofar S-Neox. In order to observe the impact of the FLP alone, waviness was removed with a Gaussian filter according to ISO 16610-61, using the cut-off length of 250 μm (Fig. 2). Subsequently, arithmetic mean surface roughness (S_a) was calculated according to ISO 25718. Scanning electron microscopy (SEM, XL30 FEG, FEI) and optical microscopy (Keyence VHX 1000) were used to analyze the LPBF surface morphology before and after *fs* laser processing.

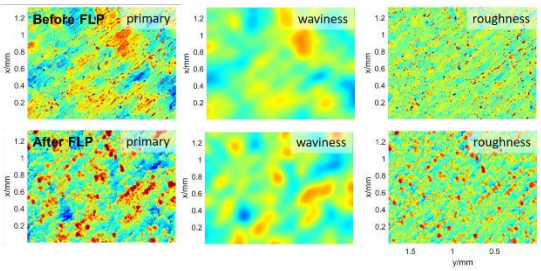

Fig. 2. Surface topography of as-built LPBF samples before (top) and after FLP (bottom)

3. Results and discussions

3.1. Effect of laser pulse energy and scanning speed

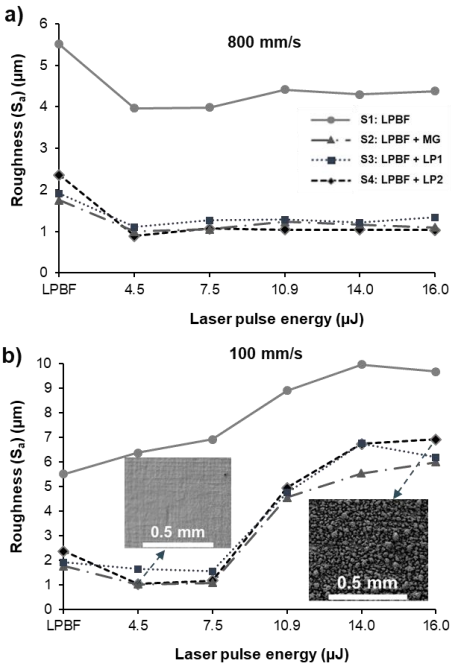

Fig. 3. Effect of laser pulse energy on surface roughness after FLP at a) ν = 100 mm/s and b) ν = 800 mm/s [N = 1]

In order to identify the optimal process parameters for better surface finish, FLP of LPBF samples was conducted at different laser pulse energies and scanning speeds. Fig. 3 shows the effect of E_p on S_a after a single FLP pass. It is evident from Fig. 3a that there is a reduction in S_a of all the samples after FLP at high scanning speed (800 mm/s). Laser polished (S3, S4) and mechanically ground (S2) samples, with initial S_a between 1.76 µm and 2.36 µm, experience a reduction in roughness up to 0.85 µm after FLP. It can be noticed that roughness remains constant with the increase in E_p at high ν (800 mm/s). However, a different behaviour was observed at low ν (100 mm/s), depending on the initial roughness. The roughness of LP and MG samples (S2-S4) initially reduces for pulse energies up to 7.5 µJ and then increases at high E_p. This effect can be attributed to the excessive energy input causing material pile-up on the processed surface during *fs* laser scanning (see SEM micrographs in Fig. 3b). Fig. 4 compares the influence of scanning speed on S_a. It is clear that higher scanning speeds typically result in a better surface finish. The difference in FLP effects on smooth samples (S2, S3 and S4) is insignificant.

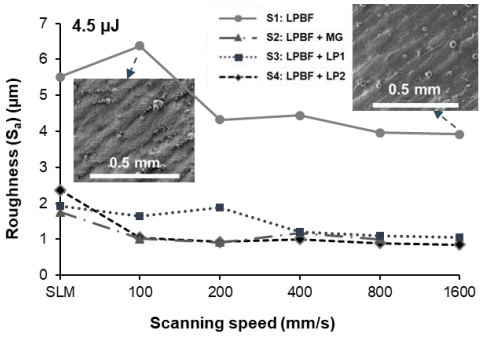

Fig. 4. Effect of FLP scanning speed on S_a [E_p = 4.5 µJ]

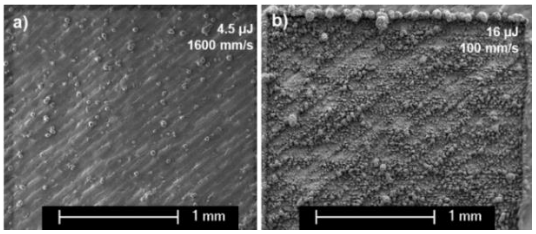

Fig. 5. Effect of FLP on as-built samples at different conditions a) low E_p and high ν and b) high E_p and low ν

For the as-built sample (S1) with an S_a of 5.5±1.3 µm, FLP reduces the roughness only marginally to the minimum of 3.9 µm for the chosen process parameters range in this experiment, whereas the effect of E_p on S_a is similar to that of other samples (Fig. 3). Despite the reduction in roughness, the LPBF melt tracks of the as-built surfaces can still be seen in Fig. 5a. It is also obvious from Fig. 5 that the spatter particles were not completely removed by FLP. Though the LPBF melt tracks are mostly ablated at higher power and lower scanning speeds, S_a is higher than the initial condition due to the material pile up on the surface by excessive energy input during FLP, as seen in Fig. 5b.

3.2. Effect of number of passes

The number of scanning passes was increased from 1 to 4 to evaluate its effect on removing the melt tracks of the as-built samples. Fig. 7 clearly indicates that multiple scanning passes have no significant effect on roughness for scanning speeds higher than 400 mm/s. At lower speeds, the melt tracks are partially removed by multiple scanning passes, leading to high S_a, as seen in Fig. 7.

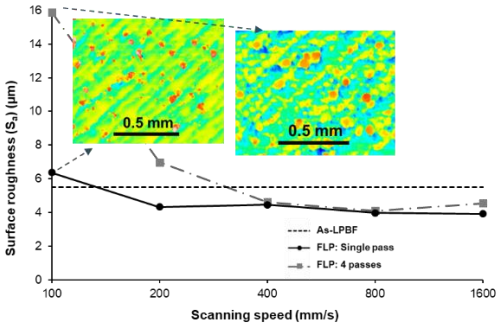

Fig. 7. Influence of number of scanning passes on as-printed sample [ν = 100 mm/s, E_p = 4.5 µJ]

3.3. Formation of LIPSS features

One of the objectives of this paper is to explore the possibility of tailoring LPBF surface textures. Fig. 6 compares the surface morphology of as-built LPBF surfaces (S1) before and after a single FLP pass with ν = 100 mm/s and E_p = 4.5 µJ. Given the constant hatch spacing of 5 µm, every spot on the surface is overlapped with at least three laser passes during FLP. As shown in Fig. 6, sub-micrometer ripples with a spatial periodicity ~ 500 nm were produced on the as-built samples despite the presence of melt-tracks and spatter particles.

Fig. 8 compares the effect of scanning speed on the surface morphology of as-built samples. Increase in scanning speed causes change in surface texture from ripples to columnar features, in the sub-micrometer scales. These results highlight the ability of FLP to fabricate LIPSS features directly on as-built LPBF surfaces irrespective of its initial surface morphology. By altering the FLP process parameters, different surface textures could be tailored using direct FLP, even with single pass scanning. However, it has to be noted that the fabrication of textures is not uniform along the surface. Interaction of laser beam with the spatter particles cause diffraction and change in the LIPSS morphology (Fig. 9), as reported earlier [12].

As a summary, it can be noted that the *fs* laser processing of as-built LPBF samples removes the microroughness and introduces LIPSS features on the surfaces. The results highlight the limitations reported

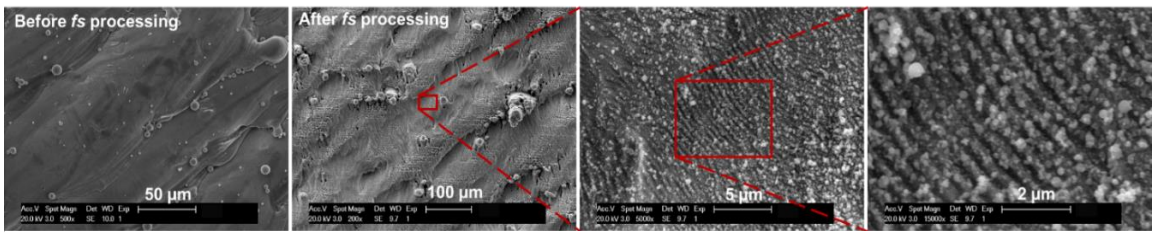

Fig. 6. LIPSS formation on as-built LPBF samples after fs laser processing [ν = 100 mm/s, E_p = 4.5 µJ; N = 1]

by the previous studies [9,12] on direct FLP. The capacity of the FLP process to remove spatter particles and LPBF melt tracks remains limited. It should be noted that the reported experiments were not conducted with *fs* laser parameters optimized for macroroughness removal. A possible strategy to address the limitations is the exploitation of multiple pass scanning strategy with varying Z offset [7]. In order to achieve fine surface finish with uniform surface textures using FLP, surface texturing should be preceded by a post-process finishing. Moreover, optimized process parameters and scanning strategies should be adopted as well.

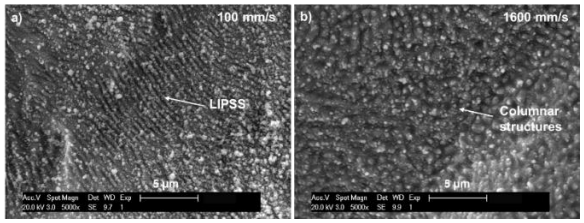

Fig. 8. Formation of surface textures a) ν = 100 mm/s, b) ν = 1600 mm/s [E_p = 4.5 µJ; N = 1]

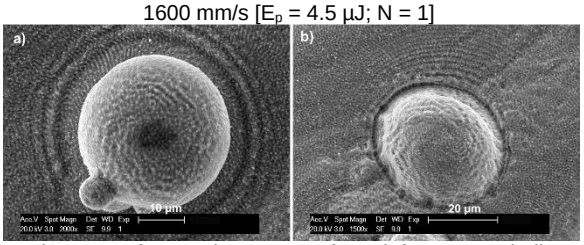

Fig. 9. Interference between surface defects on as-built surface and fs laser beam [a) E_p = 4.5 µJ, b) E_p = 16 µJ [ν = 1600 mm/s; N = 1]

The current lack of LST for LPBF parts is probably due to the fact that the surface roughness is very high, making it unsuitable for *fs* lasers to create uniform surface micro/nanotextures. However, use of finer powders and smaller layer thickness enables significantly reducing the as-built LPBF surface roughness of microscale components (R_a less than 3 µm) [2]. Therefore, LST using *fs* lasers is suitable for microscale LPBF surfaces, as similar to the formation of uniform sub-µm scale textures on laser polished LPBF samples (as shown in Fig. 10).

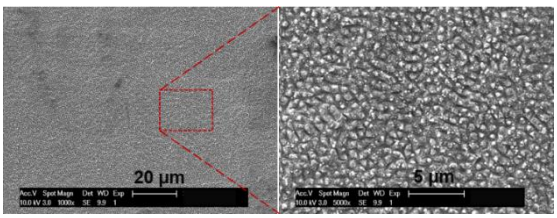

Fig. 10. Morphology of laser polished sample after FLP

4. Conclusions

This manuscript studies direct FLP of LPBF-fabricated maraging steel 300. The effects of various process parameters on the surface roughness and morphology of the processed surfaces are analyzed in detail. The following conclusions can be drawn from the results:

- Lower pulse energy and higher scanning speeds of *fs* laser processing resulted in a lower surface roughness for all the sample conditions. However, the post-processed samples (laser polished) achieve a much higher reduction in S_a (up to 64%) compared to the 30% reduction for as-built LPBF samples.
- FLP of LPBF samples impacts only the microroughness whereas the LPBF melt tracks and spatter particles were still present on the surface.
- LIPSS features with submicron wavelength (periodicity ~ 500 nm) were produced on as-built surfaces, which can also be tailored through optimizing the process parameters.

Texturing of as-built surfaces could be applicable to enhance the powder spreading capability, especially of fine powders, for microscale LPBF. Besides, at mesoscales, LST of post-processed LPBF surfaces can be used to produce functional surfaces with enhanced coating adhesion, wettability, friction, etc. Further studies will focus on optimizing the process parameters and scanning strategy to achieve surface finishing followed by texturing on as-built LPBF parts.

Acknowledgement

This research was funded by the H2020-MSCA-ITN-2016 project PAM2 [Grant no: 721383], Research Foundation Flanders (FWO) [Grant no: S009319N] (FWO-SBO project "HIPASS") and KU Leuven Bijzonder Onderzoeksfonds [Project: Laser-based hybrid manufacturing for the generation of functional surfaces (3E181039)].

References

[1] Huang, et al., "Additive Manufacturing: Current State, Future Potential, Gaps and Needs, and Recommendations," J. Manuf. Sci. Eng., 2015, 137, 14001.

[2] Nagarajan, et al., "Development of Micro Selective Laser Melting: The State of the Art and Future Perspectives," Engineering, 2019.

[3] Bhaduri, et al., "Laser Polishing of 3D Printed Mesoscale Components," Appl. Surf. Sci., 2017, 405, 29–46.

[4] Ma, et al., "Laser Polishing of Additive Manufactured Ti Alloys," Opt. Lasers Eng., 2017, 93, 171–177.

[5] Yasa, et al., "Manufacturing by Combining Selective Laser Melting and Selective Laser Erosion/Laser Re-Melting," CIRP Ann., 2011, 60, 263–266.

[6] Metelkova, et al., "Novel Strategy for Quality Improvement of Up-Facing Inclined Surfaces of LPBF Parts by Combining Laser-Induced Shock Waves and in-Situ Laser Remelting," J. Mater. Process. Technol., 2020, 290, 116981.

[7] Mingareev, et al., "Femtosecond Laser Post-Processing of Metal Parts Produced by Laser Additive Manufacturing," J. Laser Appl., 2013, 25, 052009.

[8] Nguyen, et al., "Non-Diffractive Bessel Beams for Ultrafast Laser Scanning Platform and Proof-Of-Concept Side-Wall Polishing of Additively Manufactured Parts," Micromachines, 2020, 11, 974.

[9] Worts, et al., "Surface Structure Modification of Additively Manufactured Titanium Components via Femtosecond Laser Micromachining," Opt. Commun., 2019, 430, 352–357.

[10] Ghosh, et al., "Layer-by-Layer Combination of Laser Powder Bed Fusion (LPBF) and Femtosecond Laser Surface Machining of Fabricated Stainless Steel Components," J. Manuf. Process., 2018, 35, 327–336.

[11] Vorobyev & Guo, "Direct Femtosecond Laser Surface Nano/Microstructuring and Its Applications," Laser Photon. Rev., 2013, 7, 385–407.

[12] Batal, et al., "Laser Processing of Freeform Surfaces: A New Approach Based on an Efficient Workpiece Partitioning Strategy," Int. J. Mach. Tools Manuf., 2020, 156, 103593.

[13] Metelkova, et al. "Improving the quality of up-facing inclined surfaces in laser powder bed fusion of metals using a dual laser setup." Procedia CIRP., 2020, 94, 266-269.